EFFECTS OF HEAT TREATMENT AND COMPOSITION ON BALL-MILLED MnBi AND MnBi/Co MAGNETS

T. CHAROENSUK, C. SIRISATHITKUL*
Center of Excellence in Functional Materials and Nanotechnology, Walailak University, Nakhon Si Thammarat, 80161, Thailand

The ball-milling and incorporating of cobalt (Co) are demonstrated as viable routes to produce exchange coupled hard/soft magnets from arc-melted manganese bismuth (MnBi) ingots. Properties of MnBi/Co magnets aligned by magnetic field parallel and perpendicular to the sample's plane are comparable but strongly influenced by the Mn:Bi ratio and heat treatments on the ball-milled MnBi powders. By annealing 290 °C for 40 h, the powder with Mn:Bi ratio of 2:1 leads to the highest coercivity and magnetization. In the case of MnBi sintered at 1,000 °C for 20 min, the formation of Bi_2O_3 nanowires enhances the coercivity but the magnetization is reduced with the decrease in the MnBi phase.

(Received March 17, 2018; Accepted July 4, 2018)

Keywords: Exchange coupled hard /soft magnets, MnBi, Ball-milling, Annealing, Sintering

1. Introduction

Exchange coupled hard/soft magnets are under research and development for their potential applications as rare-earth free magnets [1]. By incorporating hard magnets with soft magnetic nanostructures, the coercivity and energy product are enhanced because the soft magnetic phase impedes the magnetization reversal process of the hard magnetic phase resulting in characteristically large coercivity for permanent magnets. In [2], milling hard magnetic MnBi alloys with cobalt nanowires in liquid nitrogen gave rise to MnBi/Co nanocomposite magnets with enhanced coercivity and energy product. Magnetic properties of MnBi/Co and MnBi/$Fe_{65}Co_{35}$ nanocomposite magnets were studied by micro-magnetic simulation [3].

The low temperature phase (LTP) MnBi is a prime candidate for the hard phase in the exchange coupled hard/soft magnets with potential applications at elevated temperature due to a large positive temperature coefficient of coercivity. Its NiAs-type hexagonal crystal structure leads to high uniaxial magnetic anisotropy. This ferromagnetic phase can be converted from the paramagnetic high temperature phase (HTP) MnBi around 355 °C. However, the single-phase LTP MnBi alloy is not obtained in practice [4,5]. The peritectic solidification results in the mixed phase of MnBi, Mn and Bi. Furthermore, both Mn and Bi are susceptible to the oxidation. To produce bulk magnets, MnBi have to undergo several processing steps including grinding into powders, annealing, compacting and aligning in magnetic field [6]. The increase of the LTP was demonstrated by the annealing up to 25 h [7] and dependent on the temperature [8]. In [9], large magnetic field was applied in the solid-state reaction sintering to produce highly anisotropic MnBi magnets. The ball milling has received a great deal of attention as a pathway to refine MnBi alloyed powders. The powder refinement increases the coercivity [10, 11]. However, the prolong milling reduces the value of magnetization due to the surface oxidation [12] and Bi decomposition [13]. To prevent excessive particle agglomerations, either oleic acid as surfactants [14] or CaO as dispersants [15, 16] were included in the ball milling.

In this work, the effects of Mn:Bi ratio and heat treatment on ball-milled MnBi were demonstrated. The Mn:Bi ratio of 2:1 and 3:1 were tested to compensate the resulting segregation

*Corresponding author: chitnarong.siri@gmail.com

and unbalanced composition due to the large difference in melting points of Mn and Bi [4,5]. The MnBi powders were then used to produce MnBi/Co magnets and their magnetic properties were compared.

2. Experimental

2.1. Fabrication of MnBi and MnBi/Co magnets

Arc-melted MnBi ingots were ground and then equally separated in two portions. For the first set of samples, the temperature was increased from the room temperature to 1,000 °C with the heating rate of 60 °C/min and the samples were sintered for 20 min. After that, it was cooled down to 270 °C with the same rate and held for 20 h for the annealing. Finally, the temperature was brought down to the room temperature. The other set of sample was only annealed at 290 °C for 40 h by using the same heating and cooling rates. In addition to the different heat treatments, the effect of composition was also investigated by using ingots with varying Mn:Bi atomic ratio as 2:1 and 3:1.

After the heat treatment, the samples were milled to obtain fine MnBi powders by operating a ball-milling machine (Retsch PM100) at a speed of 200 rpm for 2 h. Stainless steel balls of 3, 4 and 5 mm in diameter were used with a balls-to-powder weight ratio of 20:1. To fabricate bulk MnBi/Co magnets, the MnBi powders were mixed with Co powders (2 μm particle size, 99.8, Aldrich) in a weight ratio of 85:15. The powders were pressed under 2500 psi uniaxial pressure for 10 min. These compacted MnBi/Co pellets were heated at 300 °C for 30 min, and then aligned in 7 kOe magnetic field for 10 min to obtain the bulk MnBi/Co magnets. Two magnetic field directions were tested, i.e. parallel to the sample's plane (y-axis) and perpendicular to the sample's plane (z-axis).

2.2. Characterization of MnBi powders and MnBi/Co magnets

Phase, morphology and magnetic properties of MnBi/Co nanocomposites were characterized. The morphology was investigated using a field emission scanning electron microscope (FESEM: Zeiss Merlin Compact). The elemental compositions were tracked by energy dispersive spectrometry (EDS: Oxford Aztec connected Zeiss Merlin Compact). The phase compositions were examined by an X-ray powder diffractometry (XRD: X'Pert MPD, Philips) with Cu-Kα radiation. The magnetic properties were measured by the vibrating sample magnetometer (VSM) up to ±10 kOe. The maximum magnetization in 10kOe is denoted as M_{max} and the magnetization in zero field is referred to as M_r.

3. Results and discussion

3.1. Phase and magnetic properties of ball-milled MnBi

From XRD patterns of annealed samples in Fig. 1a), the peaks at 28.14°, 38.14°, 42.20°, 51.13°, 51.49°, 68.68°, 52.14° and 29.21° respectively correspond to the (101), (102), (110), (103), (201), (211), (112) and (002) diffraction planes of MnBi (Reference: 03-065-8164 bismuth manganese). However, the single phase MnBi is not obtained and the Mn, Bi as well as impurity phases are also formed similar to the literature [4,5]. By comparing samples with Mn:Bi of 2:1 and 3:1, the XRD peaks are located at the same positions but relative peak intensities are different. The sintered samples in Fig. 1b) exhibit higher Bi peak at 27.16°, 39.62°, 48.70°, 64.51° and 62.18° (Reference: 01-085-1329 bismuth) at the expense of the MnBi phase.

From hysteresis loops of ball-milled MnBi shown in Fig. 2, magnetic parameters can be listed. The coercivity and remanent magnetization summarized in Table 1 are much lower than those reported in literature in the past few years [10, 11, 16-18]. Nevertheless, the effects of heat treatment and composition are demonstrated in this work. The largest magnetization (6.1 emu/g) is obtained after milling in the case of annealed powders with Mn:Bi ratio of 2:1 but this sample does not exhibit the largest coercivity. Interestingly, the larger value (538.5 Oe) is obtained in the sintered powders with Mn:Bi ratio of 3:1 which is likely attributed to the increased in Bi phase impeding the magnetization reversal process of MnBi. EDS spectra, not shown here, also suggest the existence of Bi_2O_3 phase which is not clearly detected by XRD. The sintering at 1,000 °C apparently leads to the segregation and oxidation of Bi.

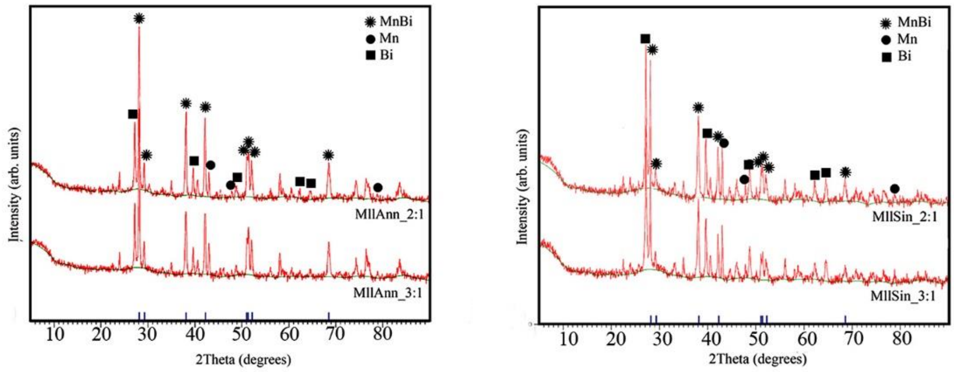

(a) *(b)*

Fig. 1. XRD patterns of (a) annealed and (b) sintered samples prepared with Mn:Bi ratio of 2:1 and 3:1 after the ball-milling.

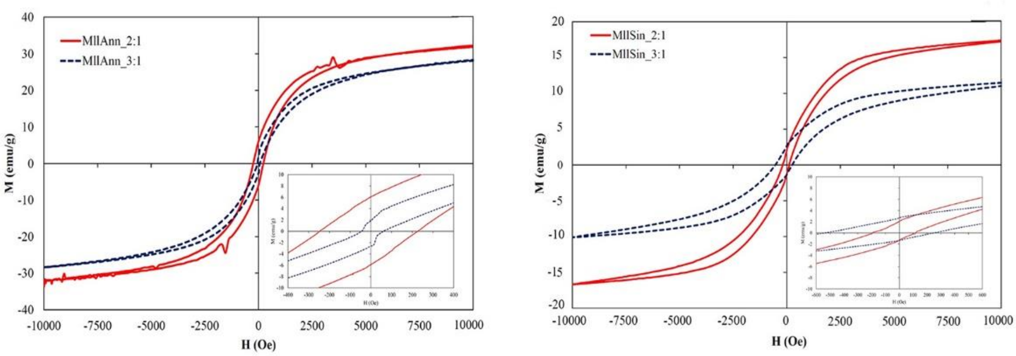

(a) *(b)*

Fig. 2. M-H curves of (a) annealed and (b) sintered samples prepared with Mn:Bi ratio of 2:1 and 3:1 after the ball-milling. Insets are magnified portions at low fields up to ±400 Oe.

3.2. Morphology and magnetic properties of MnBi/Co magnets

FESEM images of bulk MnBi/Co magnets prepared by using annealed and sintered powders with Mn:Bi ratio of 2:1 and 3:1 are shown in Fig. 3. All samples have compact morphology with some pores between microclusters. The ball-milling reduces the grain size of annealed and sintered MnBi and these fine powders form agglomerates with Co powders into microclusters due to magnetic interaction. Moreover, Figs. 3c) and 3d) reveal needle-like feature in magnets prepared with sintered powders. These nanowires are likely due to the segregation and oxidation of Bi. Similar Bi_2O_3 nanowires were reported in [19].

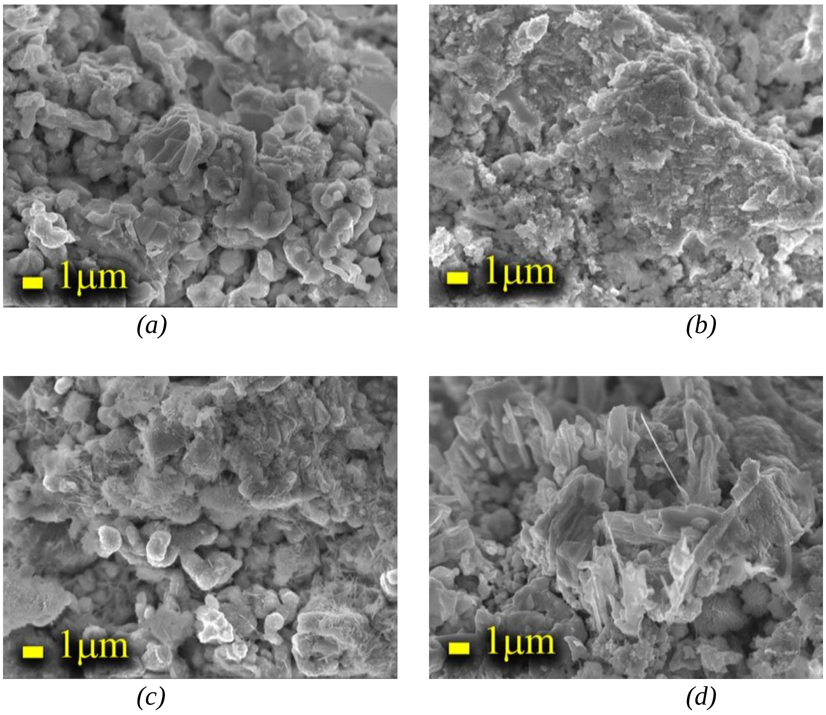

Fig. 3. FESEM images of MnBi/Co magnets from annealed samples prepared with Mn:Bi ratio of a) 2:1 and b) 3:1; sintered samples prepared with Mn:Bi ratio of c) 2:1, d) 3:1.

Fig. 4 and Table 1 compare magnetic properties of MnBi/Co magnets using different ball-milled MnBi powders and directions of magnetic alignment. Overall, the magnetic properties of MnBi/Co magnets exhibit small variations with the direction of magnetic alignment. Importantly, the coercivity and magnetization of magnets become less sensitive to the composition and heat treatment. The difference in magnetization of MnBi/Co magnets is reduced compared to those among the MnBi powders. The varying coercivity of 146.1-256.5 Oe in the MnBi/Co magnets is in a much smaller range than 45.3-538.5 Oe in the ball-milled powders. The result implies that the effect of Bi_2O_3 nanowires is more significant than that of Co. The magnets prepared from annealed powders with Mn:Bi ratio of 2:1 have the highest coercivity and magnetization. The reduction in magnetization in the case of sintered powders is attributed to the reduction in MnBi phase observed by XRD. Nevertheless, the Bi and Bi_2O_3 phases observed by XRD, EDS and FESEM in the case of sintered powders may impede the magnetization reversal process resulting in considerable coercivity.

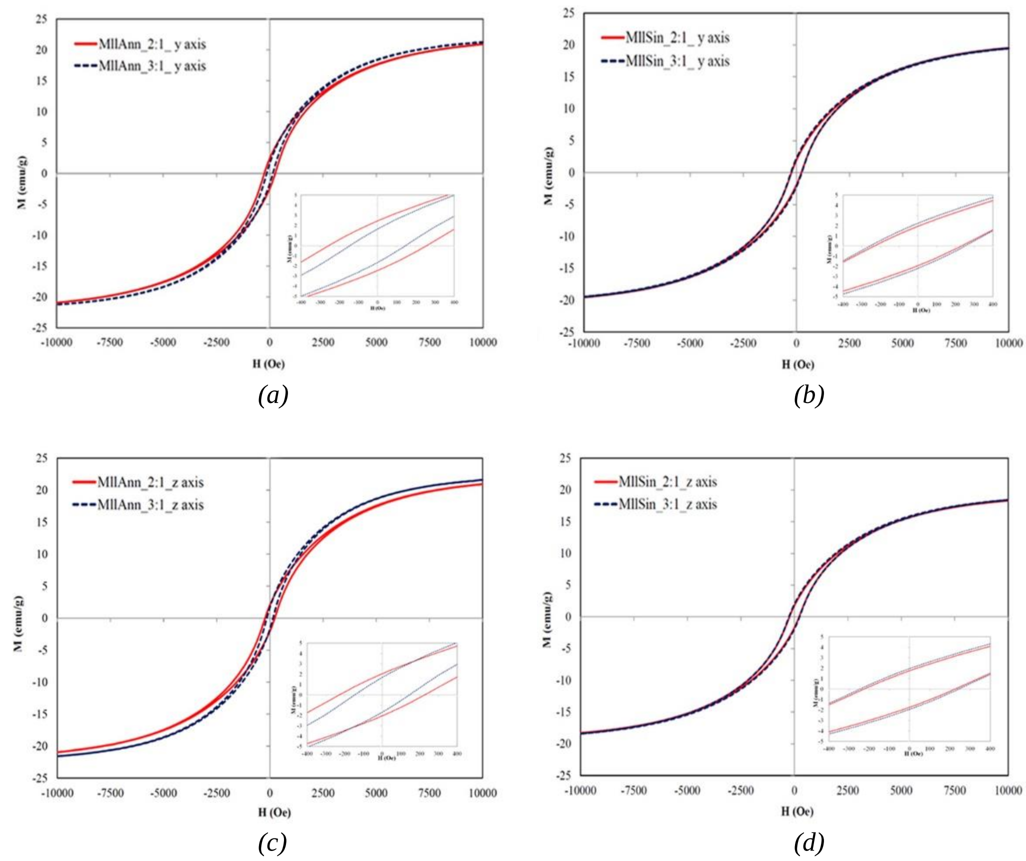

Fig. 4. M-H curves of MnBi/Co magnets prepared by using a) annealed and b) sintered powders with Mn:Bi ratio of 2:1 and 3:1 and aligned in magnetic field parallel to the sample's plane (y-axis); c) annealed and d) sintered powders with Mn:Bi ratio of 2:1 and 3:1 and aligned in magnetic field perpendicular to the sample's plane (z-axis). Insets are magnified portions at low fields up to ±400 Oe.

Table 1. Magnetic properties of ball-milled MnBi and MnBi/Co magnets.

Sample	H_c (Oe)		M_r (emu/g)		M_{max} (emu/g)	
	Mn:Bi 2:1	**Mn:Bi 3:1**	**Mn:Bi 2:1**	**Mn:Bi 3:1**	**Mn:Bi 2:1**	**Mn:Bi 3:1**
Milled MnBi						
-annealed powder	246.9	45.3	6.1	1.9	31.7	28.2
-sintered powder	193.2	538.5	2.0	2.7	17.4	11.5
MnBi/Co						
Aligned in y-axis						
-annealed powder	256.5	146.1	2.4	1.6	20.9	21.3
-sintered powder	233.5	254.2	2.0	2.2	19.5	19.5
MnBi/Co						
Aligned in z-axis						
-annealed powder	228.0	147.0	2.0	1.7	21.0	21.6
-sintered powder	228.2	246.1	1.7	1.9	18.3	18.4

4. Conclusions

The Mn:Bi ratio and heat treatments strongly affected coercivity and magnetization of ball-mill MnBi powders. However, the difference in magnetic properties were less marked in MnBi/Co magnets. The MnBi/Co magnets prepared from annealed MnBi powders with Mn:Bi ratio of 2:1 exhibited the largest coercivity and magnetization. The use of sintered powders decreased the magnetization due to the formation of Bi and Bi_2O_3 phases at the expense of LTP

MnBi. On the other hand, the coercivity tended to increase by the inclusion of Bi_2O_3 nanowires. These magnetic properties showed small variations with the direction of magnetic alignment.

Acknowledgements

This work is financially supported by Walailak University (Grant No. WU60122) and Thailand Excellent Center in Physics (ThEP-60-PIP-WU3). We would like to thank Mr. Praiwan Kerdthongmee of Walailak University for the electromagnet, Asst. Prof. Dr. Pongsakorn Jantaratana of Kasetsart University for the VSM, Asst. Prof. Dr. Boonrat Lohwongwatana and Dr. Atchara Khamkongkaeo of Chulalongkorn University for the arc-melt facilities.

References

[1] N. Poudyal, J. P. Liu, Journal of Physics D: Applied Physics **46**, 043001 (2013).
[2] T. X. Nguyen, O. K. T. Vuong, H. T. Nguyen, V. V. Nguyen, Journal of Electronic Materials **46**(6), 3359 (2017).
[3] Y. Q. Li, M. Yue, T. Wang, Q. Wu, D. T. Zhang, Y. Gao, Journal of Magnetism and Magnetic Materials **393**, 484 (2015).
[4] J. Cui, J. P. Choi, E. Polikarpov, M. E. Bowden, W. Xie, G. Li, Z. Nie, N. Zarkevich, M. J. Kramer, D. Johnson, Acta Materialia **79**, 374 (2014).
[5] K. Isogai, M. Matsuura, N. Tezuka, S. Sugimoto, Materials Transactions **54**, 1673 (2013).
[6] V. V. Nguyen, T. X. Nguyen, Physica B **532**, 103 (2018).
[7] B. B. Li, Y. L. Ma, B. Shao, C. H. Li, D. M. Chen, J. C. Sun, Q. Zheng, X. G. Yin, Physica B **530**, 322 (2018).
[8] N. R. Christopher, N. Singh, S. K. Singh, B. Gahtori, S. K. Mishra, A. Dar, V. P. S. Awana, Journal of Superconductivity and Novel Magnetism **26**, 3161 (2013).
[9] Y. Mitsui, R. Y. Umetsu, K. Koyama, K. Watanabe, Journal of Alloys and Compounds **615**, 131 (2014).
[10] W. Xie, E. Polikarpov, J. P. Choi, M. E. Bowden, K. Sun, J. Cui, Journal of Alloys and Compounds **680**, 1 (2016).
[11] S. Kim, H. Moon, H. Jung, S.-M. Kim, H.-S. Lee, H. Choi-Yim, W. Lee, Journal of Alloys and Compounds **708**, 1245 (2017).
[12] A. M. Gabay, G. C. Hadjipanayis, JOM **67**, 1329 (2015).
[13] V. V. Nguyen, T. X. Nguyen, Journal of Electronic Materials **46**(6), 3333 (2017).
[14] K. Kanari, C. Sarafidis, M. Gjoka, D. Niarchos, O. Kalogirou, Journal of Magnetism and Magnetic Materials **426**, 691 (2017).
[15] N. V. Rama Rao, G. C. Hadjipanayis, Journal of Alloys and Compounds **616**, 319 (2014).
[16] A. M. Gabay, G. C. Hadjipanayis, AIP Advances **7**, 056217 (2017).
[17] N. Poudyal, X. Liu, W. Wang, V. V. Nguyen, Y. Ma, K. Gandha, K. Elkins, J. P. Liu, K. Sun, M. J. Kramer, J. Cui, AIP Advances **6**, 056004 (2016).
[18] Y.-C. Chen, S. Sawatzki, S. Ener, H. Sepehri-Amin, A. Leineweber, G. Gregori, F. Qu, S. Muralidhar, T. Ohkubo, K. Hono, O. Gutfleisch, H. Kronmüller, G. Schütz, E. Goering, AIP Advances **6**, 125301 (2016).
[19] C. M. B. Hincapié, M. J. P. Cárdenas, J. E. A. Orjuela, E. R. Parra, J. J. O. Florez, Dyna, **79**(176), 139-148 (2012).